

Electronic Supplementary Information

How to not build a cage: endohedral functionalization of polyoxometalate-based metal–organic polyhedra

Ji Guo,^a Qing Chang,^a Zhiwei Liu,^a Yangming Wang,^a Chuanhong Liu,^a Mou Wang,^a Danmeng Huang,^a Guanying Chen,^a Hongmei Zhao,^b Wei Wang,^{*c} and Xikui Fang^{*a}

^a MIT Key Laboratory of Critical Materials Technology for New Energy Conversion and Storage, School of Chemistry and Chemical Engineering, Harbin Institute of Technology, Harbin 150001, China. E-mail: xkfang@hit.edu.cn

^b State Key Laboratory of Information Photonics and Optical Communications, School of Science, Beijing University of Posts and Telecommunications, Beijing 100876, China

^c CAS Key Laboratory of Design and Assembly of Functional Nanostructures, and Fujian Provincial Key Laboratory of Nanomaterials, Fujian Institute of Research on the Structure of Matter, Chinese Academy of Sciences; Xiamen Institute of Rare Earth Materials, Haixi Institutes, Chinese Academy of Sciences, Xiamen, Fujian, 361021, China. E-mail: wangwei@fjirsm.ac.cn

Table of Contents

Instruments and Physical Measurements	S2
Infrared spectra (Fig. S1–S3)	S3
Thermogravimetric analyses (Fig. S4–S7)	S4
UV spectra (Fig. S8)	S6
¹ H and ³¹ P NMR spectra of 2 and 3 (Fig. S9–S11)	S7
X-ray photoelectron spectroscopy (Fig. S12)	S8
Single-Crystal X-Ray Structure Determination	S9
Crystal data for 1a (Table S1)	S9
Crystal data for 1b (Table S2)	S10
The optimized interior structure of 1b and π - π stacking interactions (Fig. S13)	S11
Crystal data for 2 (Table S3)	S12
Crystal data for 3 (Table S4)	S13
Bond Valence Sum (BVS) Calculations (Tables S5–S8)	S14
References	S17

Instruments and Physical Measurements

General: IR spectra (KBr pellets) were collected on a Thermo Nicolet Avatar 360 FTIR spectrophotometer. Atmosphere compensation (CO₂ and H₂O) and baseline corrections were carried out after spectrum collection. ¹H NMR spectra and ³¹P NMR were collected on a Bruker Avance III 400 MHz NMR instrument. Elemental analyses were performed on a Vario EL III analyzer (for C, H, N) and Perkin-Elmer ICP–OES (for P, S, and V). The UV-visible spectra were recorded on a Perkin-Elmer Lambda 750 spectrophotometer. Thermal gravimetric analyses were measured with a TA Instruments SDT-Q600 thermal analysis system under N₂ flow with 10 °C/min heating. X-ray photoelectron spectroscopy (XPS) measurements were performed by using a PHI 5700 ESCA system equipped with Al K α (1486.6 eV) X-ray source. The density functional theory calculations were performed at the level of B3LYP/3-21G using the Gaussian 09^{S1} package.

Single-crystal X-ray diffraction: The single-crystal X-ray diffraction data were collected using a Bruker D8 Quest X-ray diffractometer equipped with an Incoatec Microfocus Mo Source (I μ S 3.0, $\lambda = 0.71071 \text{ \AA}$) and a PHOTON II CPAD detector. Suitable crystals were coated with Paratone N oil, suspended on a small fiber loop, and placed in a 173(2) K cooled nitrogen stream from Oxford Cryosystems Cryostream equipment. For all cases, the raw data were processed with the Bruker APEX3 software package. The data were solved by intrinsic phasing methods^{S2} and the refinement was done by full-matrix least squares on F^2 using SHELXL^{S3} (2018/3). Hydrogen atoms on the organic linkers, terminal methoxyl groups, the interior organophosphonate units and the tetramethylammonium counter ions are placed geometrically and refined using a riding model; PART, SIMU, DELU, ISOR and AFIX 66 instructions were used to deal with the disorder of interior phenyl groups on the phosphonates. The SQUEEZE option of PLATON^{S4} was used to model the contribution of disordered solvent molecules and counter ions to the reflection intensities.

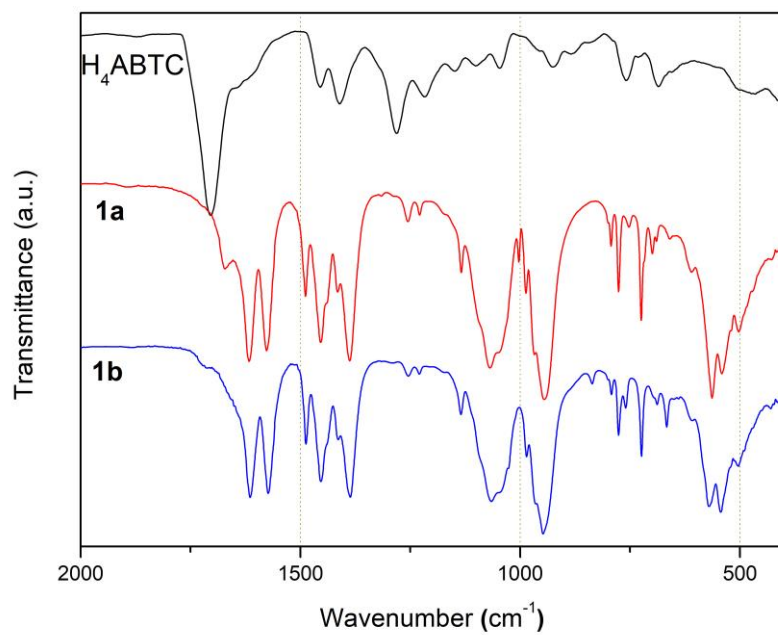


Fig. S1 Comparison of the IR spectra of H₄ABTC, **1a** and **1b**.

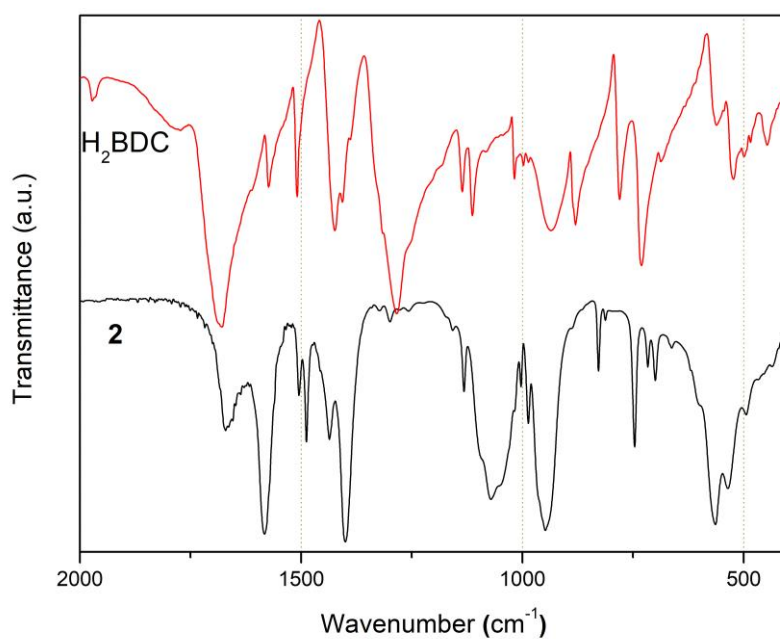


Fig. S2 Comparison of the IR spectra of H₂BDC and **2**.

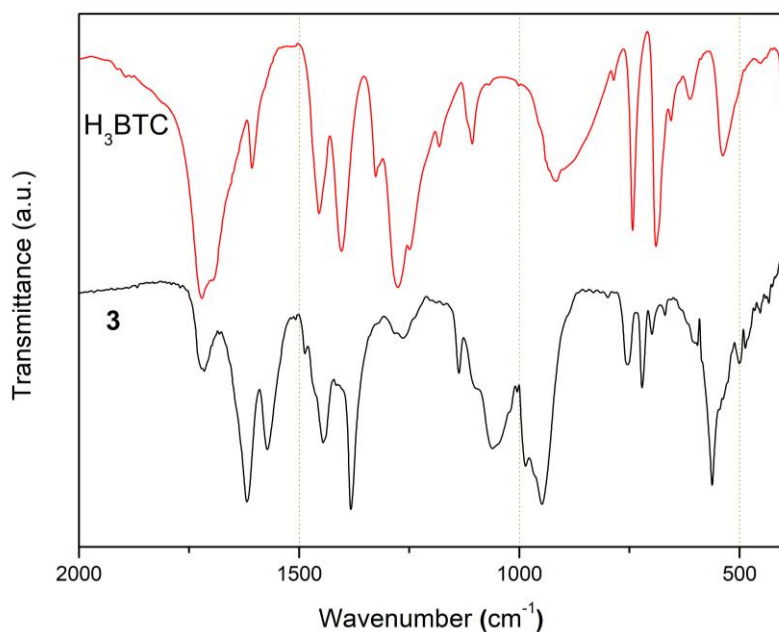


Fig. S3 Comparison of the IR spectra of H₃BTC and **3**.

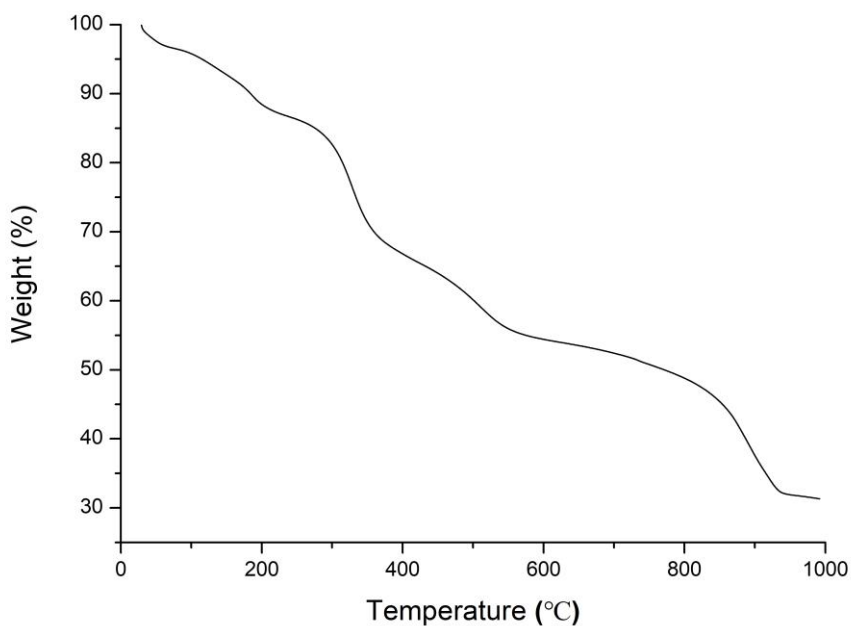


Fig. S4 Thermogravimetric analysis trace of **1a**. The weight loss of 3.5% between 30 and 80 °C is associated with the loss of 12 methanol molecules (calcd. 3.4%); the weight loss of 8.0% between 80 and 200 °C is associated with the loss of 12 N,N-dimethylformamide molecules (calcd. 7.7%); the weight loss of 20.0% between 200 and 375 °C is attributed to the loss of 72 methoxy groups (calcd.19.8%).

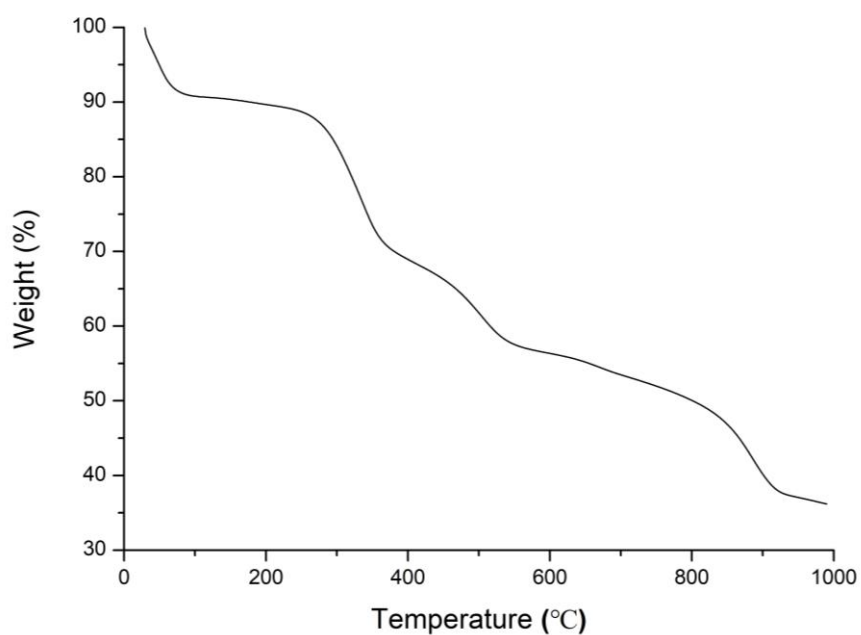


Fig. S5 Thermogravimetric analysis trace of **1b**. The weight loss of 8.7% between 30 and 80 °C is associated with the loss of 32 methanol molecules (calcd. 8.6%); the weight loss of 1.6% between 80 and 200 °C is associated with the loss of 3 N,N-dimethylformamide molecules (calcd. 1.8%); the weight loss of 19.28% between 200 and 375 °C is attributed to the loss of 72 methoxy groups (calcd. 18.8%).

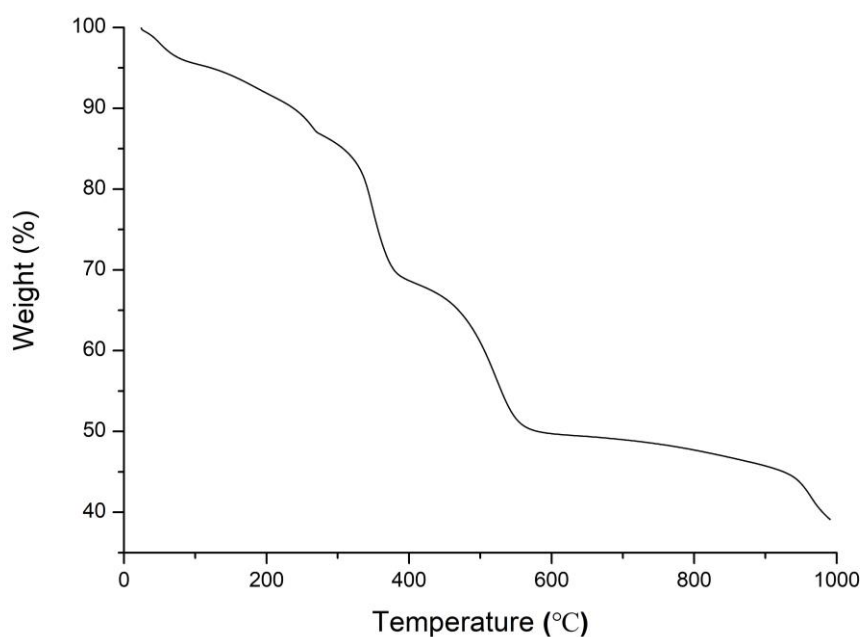


Fig. S6 Thermogravimetric analysis trace of **2**. The weight loss of 3.9% between 30 and 80 °C is associated with the loss of 7 methanol molecules (calcd. 4.1%); the weight loss of 4.2% between 80 and 200 °C is associated with the loss of 3 N,N-dimethylformamide molecules (calcd. 4.1%); the weight loss of 21.7% between 200 and 375 °C is attributed to the loss of 36 methoxy groups (calcd. 20.8%).

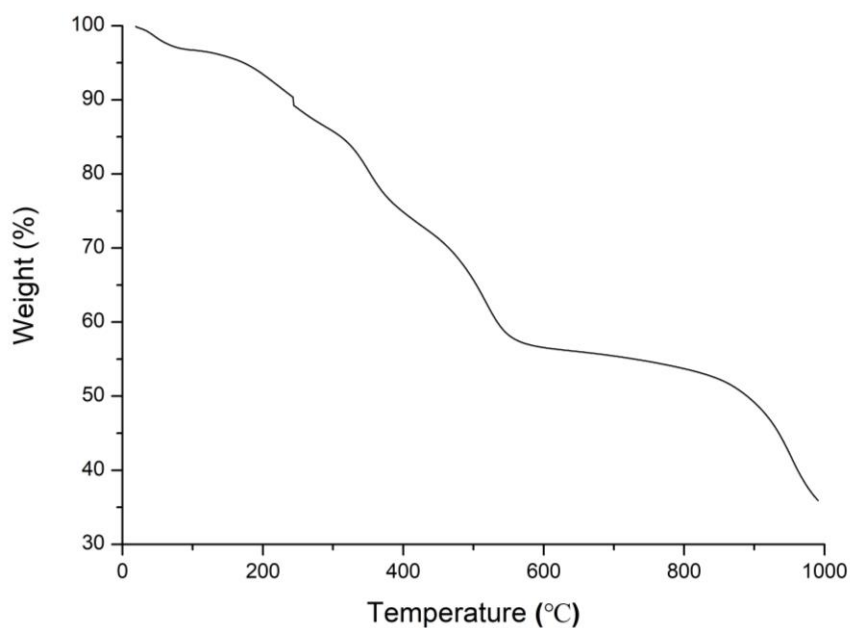


Fig. S7 Thermogravimetric analysis trace of **3**. The weight loss of 3.0% between 30 and 80 °C is associated with the loss of 11 methanol molecules (calcd. 3.0%); the weight loss of 3.6% between 80 and 200 °C is associated with the loss of 6 N,N-dimethylformamide molecules (calcd. 3.7%); the weight loss of 20.1% between 200 and 420 °C is attributed to the loss of 80 methoxy groups (calcd. 21.2%)

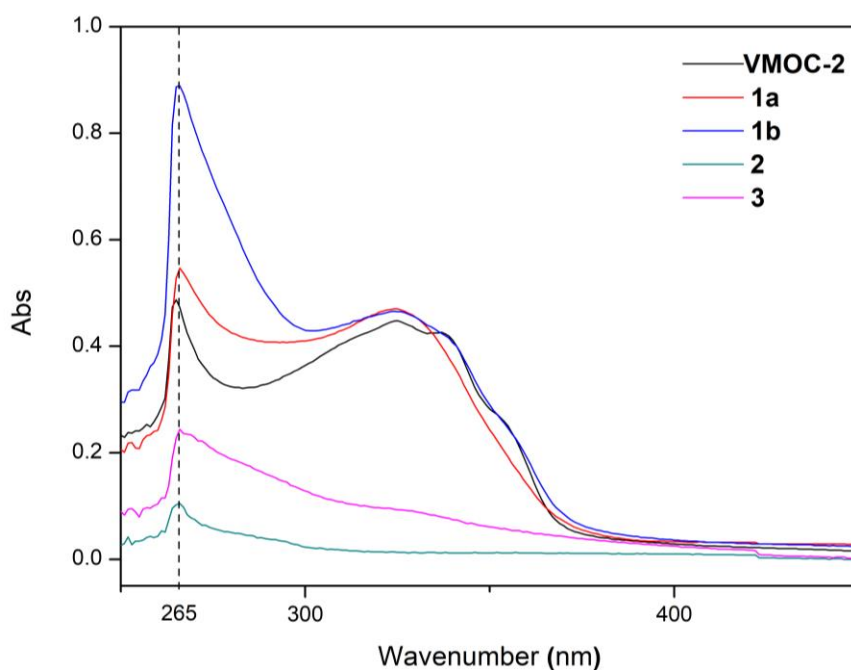


Fig. S8 UV-Vis absorption spectra of **VMOC-2**, **1a**, **1b**, **2** and **3** (2.5×10^{-6} mol L⁻¹). All samples of the unfunctionalized and functionalized cubic cages (**VMOC-2**, **1a**, **1b**) show a pronounced absorption band at ~320 nm, characteristic of the $\pi \rightarrow \pi^*$ transition of *trans*-azobenzene units in ABTC.

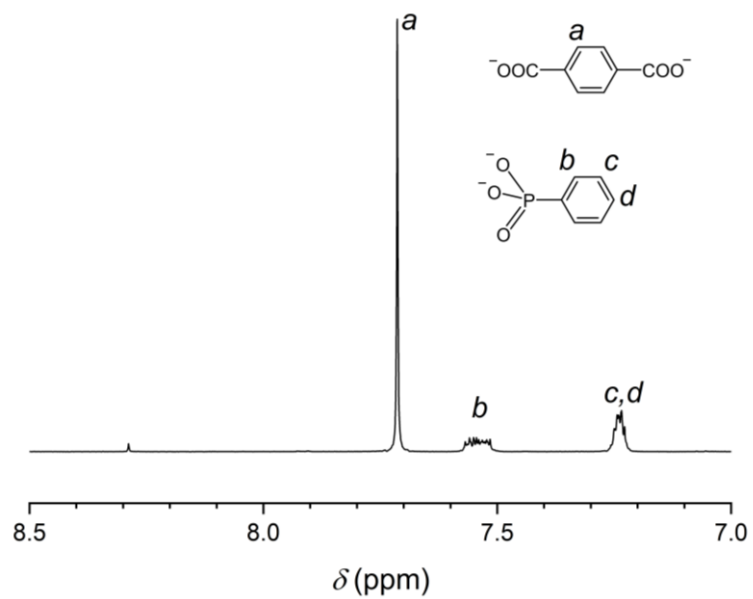


Fig. S9 ^1H NMR spectrum of a base-digested sample of **2** (400 MHz, NaOD/D₂O, 293 K).

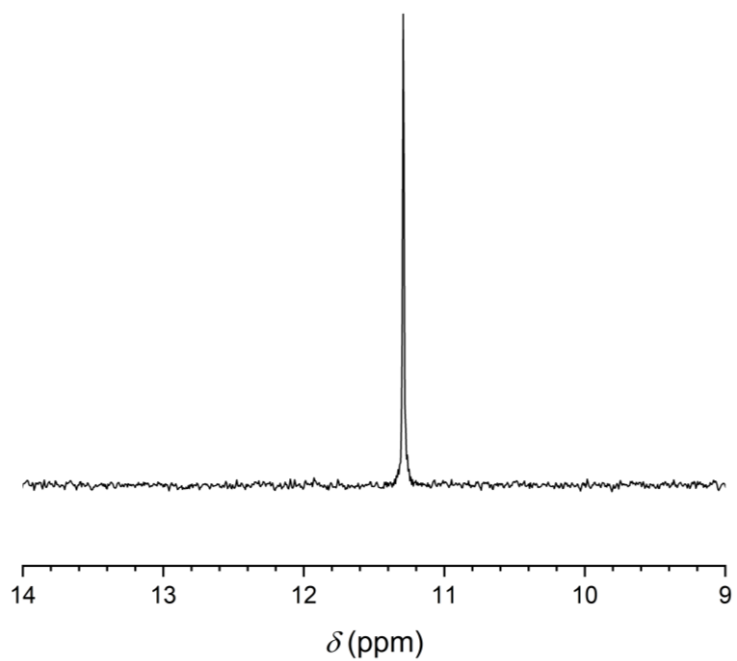


Fig. S10 ^{31}P NMR spectrum of a base-digested sample of **2** (400 MHz, NaOD/D₂O, 293 K).

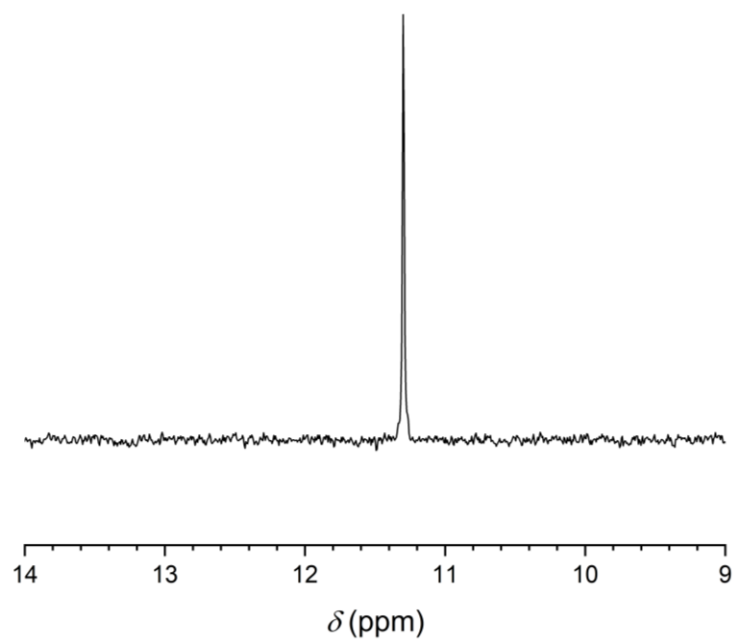


Fig. S11 ^{31}P NMR spectrum of a base-digested sample of **3** (400 MHz, NaOD/D₂O, 293 K).

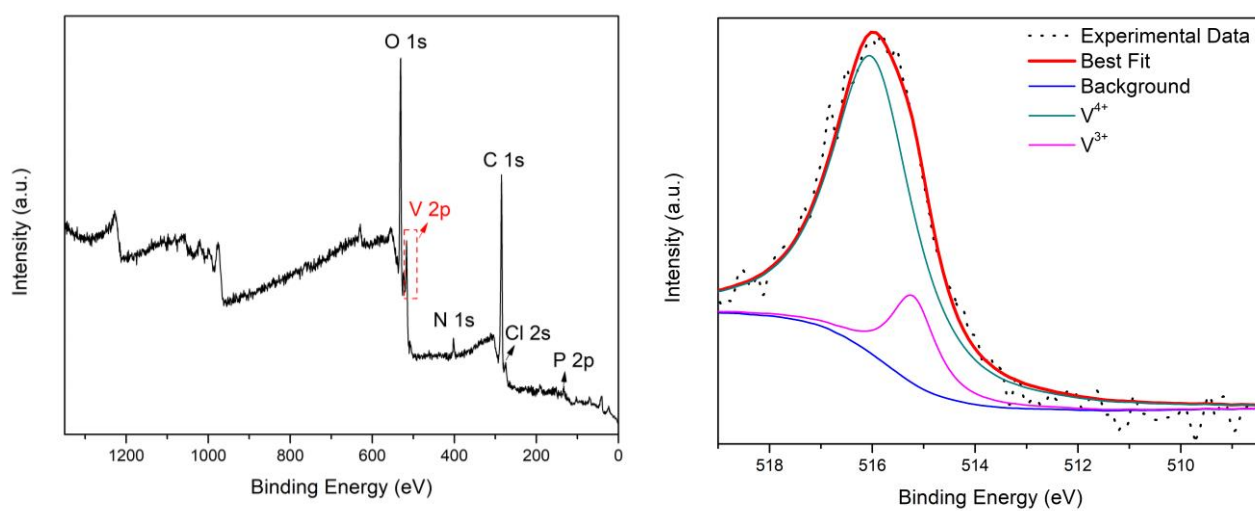


Fig. S12 X-ray photoelectron spectroscopy (XPS) of **3**. The integral area ratio for V⁴⁺(2p_{3/2}) and V³⁺(2p_{3/2}) is 6.14, agreeing with their ratio (48:8) in the crystal structure of **3**.

Single-Crystal X-ray Structure Determination

Table S1 Crystal data and structure refinement for **1a** (CCDC deposit number: 2054446).

	1a
Empirical formula	C ₃₂₈ H ₆₁₆ N ₄₀ O ₂₁₆ P ₈ V ₄₈
Formula weight	11269.45
Temperature	173(2) K
Wavelength	0.71073 Å
Crystal system	Monoclinic
Space group	<i>P</i> 2 ₁ / <i>n</i>
Unit cell dimensions	<i>a</i> = 24.986(2) Å <i>α</i> = 90 ° <i>b</i> = 41.240(4) Å <i>β</i> = 108.986(2) ° <i>c</i> = 25.1687(19) Å <i>γ</i> = 90 °
Volume	24524(4) Å ³
<i>Z</i>	2
Density (calculated)	1.526 Mg/m ³
Absorption coefficient	0.986 mm ⁻¹
<i>F</i> (000)	11632
Crystal size	0.230 x 0.150 x 0.090 mm ³
Theta range for data collection	2.153 to 26.533 °
Index ranges	-31 ≤ <i>h</i> ≤ 29, -50 ≤ <i>k</i> ≤ 51, -28 ≤ <i>l</i> ≤ 28
Reflections collected	106753
Independent reflections	48197 [<i>R</i> (int) = 0.0561]
Completeness to <i>θ</i> = 25.242 °	96.3 %
Absorption correction	Semi-empirical from equivalents
Refinement method	Full-matrix least-squares on <i>F</i> ²
Data / restraints / parameters	48197 / 567 / 2176
Goodness-of-fit on <i>F</i> ²	1.100
Final <i>R</i> indices [<i>I</i> > 2σ(<i>I</i>)]	<i>R</i> ₁ = 0.0751, <i>wR</i> ₂ = 0.2301
<i>R</i> indices (all data)	<i>R</i> ₁ = 0.1038, <i>wR</i> ₂ = 0.2506
Largest diff. peak and hole	2.727 and -1.016 e.Å ⁻³

**R*₁ = Σ||*F*₀|-|*F*_c||/Σ|*F*₀|, *wR*₂ = [Σ[*w*(*F*₀²-*F*_c²)²]/Σ[*w*(*F*₀²)]^{1/2}

Table S2 Crystal data and structure refinement for **1b** (CCDC deposit number: 2054447).

1b	
Empirical formula	C ₃₆₉ H ₆₆₅ N ₃₁ O ₂₂₇ P ₈ V ₄₈
Formula weight	11861.16
Temperature	173(2) K
Wavelength	0.71073 Å
Crystal system	Monoclinic
Space group	<i>P</i> 2 ₁ / <i>n</i>
Unit cell dimensions	<i>a</i> = 24.986(16) Å <i>α</i> = 90 ° <i>b</i> = 42.565(3) Å <i>β</i> = 109.572(2) ° <i>c</i> = 25.2167(18) Å <i>γ</i> = 90 °
Volume	25269(3) Å ³
<i>Z</i>	2
Density (calculated)	1.559 Mg/m ³
Absorption coefficient	0.962 mm ⁻¹
<i>F</i> (000)	12272
Crystal size	0.250 x 0.240 x 0.240 mm ³
Theta range for data collection	2.180 to 23.280 °
Index ranges	-27 ≤ <i>h</i> ≤ 26, -47 ≤ <i>k</i> ≤ 47, - 28 ≤ <i>l</i> ≤ 28
Reflections collected	104767
Independent reflections	36203 [<i>R</i> (int) = 0.0914]
Completeness to <i>θ</i> = 23.280 °	99.5 %
Absorption correction	Semi-empirical from equivalents
Refinement method	Full-matrix least-squares on <i>F</i> ²
Data / restraints / parameters	36203 / 91 / 1867
Goodness-of-fit on <i>F</i> ²	1.030
Final <i>R</i> indices [<i>I</i> > 2σ(<i>I</i>)]	<i>R</i> ₁ = 0.1215, <i>wR</i> ₂ = 0.2960
<i>R</i> indices (all data)	<i>R</i> ₁ = 0.2255, <i>wR</i> ₂ = 0.3816
Largest diff. peak and hole	1.167 and -0.734 e.Å ⁻³

**R*₁ = Σ||*F*_o|-|*F*_c||/Σ|*F*_o|, *wR*₂ = [Σ[*w*(*F*_o²-*F*_c²)²]/Σ[*w*(*F*_o²)²]^{1/2}

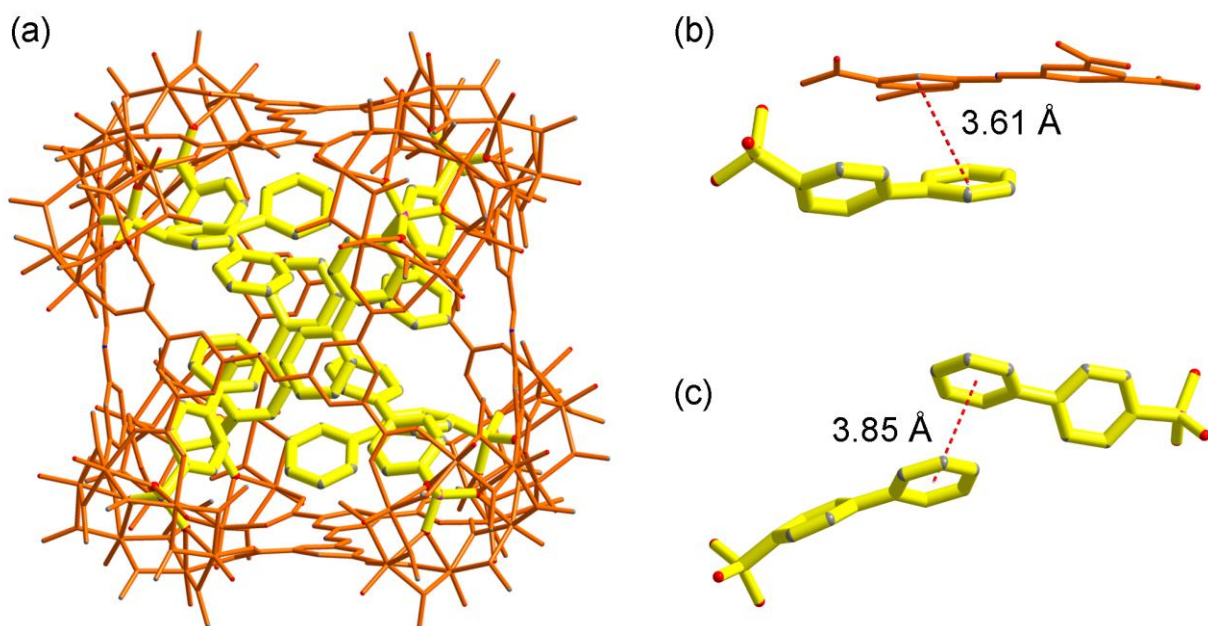


Fig. S13 (a) The optimized interior structures of **1b**, with hydrogen atoms omitted for clarity. The outer shell structure (in orange) were determined by the X-ray single-crystal structure analysis, while the interior biphenyl-4-phosphonates (in yellow) were based on an optimized molecular model (B3LYP/3-21G). Representative π - π stacking interactions between the ABTC panels and the biphenylphosphonate units (b) and those between the interior biphenylphosphonate groups themselves (c) are shown on the right.

Table S3 Crystal data and structure refinement for **2** (CCDC deposit number: 2054448).

2	
Empirical formula	C ₁₅₆ H ₂₉₇ N ₁₁ O ₁₀₆ P ₄ V ₂₄
Formula weight	5369.47
Temperature	173(2) K
Wavelength	0.71073 Å
Crystal system	Monoclinic
Space group	<i>P</i> 2 ₁ / <i>m</i>
Unit cell dimensions	<i>a</i> = 27.776(3) Å <i>α</i> = 90 ° <i>b</i> = 32.560(3) Å <i>β</i> = 105.890(3) ° <i>c</i> = 36.610(3) Å <i>γ</i> = 90 °
Volume	31844(5) Å ³
<i>Z</i>	4
Density (calculated)	1.120 Mg/m ³
Absorption coefficient	0.755 mm ⁻¹
<i>F</i> (000)	11080
Crystal size	0.180 x 0.180 x 0.150 mm ³
Theta range for data collection	1.963 to 23.351 °
Index ranges	-30 ≤ <i>h</i> ≤ 30, -36 ≤ <i>k</i> ≤ 36, - 40 ≤ <i>l</i> ≤ 40
Reflections collected	496865
Independent reflections	46725 [<i>R</i> (int) = 0.1035]
Completeness to <i>θ</i> = 23.351 °	99.0 %
Absorption correction	Semi-empirical from equivalents
Refinement method	Full-matrix least-squares on <i>F</i> ²
Data / restraints / parameters	46725 / 409 / 2271
Goodness-of-fit on <i>F</i> ²	1.048
Final <i>R</i> indices [<i>I</i> > 2σ(<i>I</i>)]	<i>R</i> ₁ = 0.0721, <i>wR</i> ₂ = 0.2000
<i>R</i> indices (all data)	<i>R</i> ₁ = 0.0906, <i>wR</i> ₂ = 0.2115
Largest diff. peak and hole	0.984 and -0.552 e.Å ⁻³

**R*₁ = Σ||*F*_o|-|*F*_c||/Σ|*F*_o|, *wR*₂ = [Σ[w(*F*_o²-*F*_c²)²]/Σ[w(*F*_o²)²]^{1/2}

Table S4 Crystal data and structure refinement for **3** (CCDC deposit number: 2054449).

3	
Empirical formula	C ₃₀₉ H ₆₁₀ ClN ₂₃ O ₂₄₅ P ₈ V ₅₆
Formula weight	11704.01
Temperature	173(2) K
Wavelength	0.71073 Å
Crystal system	Monoclinic
Space group	C2/m
Unit cell dimensions	$a = 39.096(7)$ Å $\alpha = 90^\circ$ $b = 26.059(5)$ Å $\beta = 113.642(4)^\circ$ $c = 29.242(5)$ Å $\gamma = 90^\circ$
Volume	27292(9) Å ³
Z	2
Density (calculated)	1.424 Mg/m ³
Absorption coefficient	1.022 mm ⁻¹
F(000)	12020
Crystal size	0.330 x 0.300 x 0.280 mm ³
Theta range for data collection	2.234 to 23.410 °
Index ranges	-43 ≤ h ≤ 43, -29 ≤ k ≤ 28, - 31 ≤ l ≤ 32
Reflections collected	114135
Independent reflections	20281 [<i>R</i> (int) = 0.1296]
Completeness to $\theta = 23.410^\circ$	98.9 %
Absorption correction	Semi-empirical from equivalents
Refinement method	Full-matrix least-squares on <i>F</i> ²
Data / restraints / parameters	20281 / 414 / 1226
Goodness-of-fit on <i>F</i> ²	1.081
Final <i>R</i> indices [<i>I</i> > 2σ(<i>I</i>)]	<i>R</i> ₁ = 0.1330, <i>wR</i> ₂ = 0.3307
<i>R</i> indices (all data)	<i>R</i> ₁ = 0.2048, <i>wR</i> ₂ = 0.3952
Largest diff. peak and hole	1.421 and -1.147 e.Å ⁻³

* $R_1 = \sum ||F_o| - |F_c|| / \sum |F_o|$, $wR_2 = [\sum [w(F_o^2 - F_c^2)^2] / \sum [w(F_o^2)^2]]^{1/2}$

Bond Valence Sum (BVS) Calculations:

For determination of the oxidation states of metal centers and the protonation states of oxygen sites, BVS calculations were carried out using the method of I. D. Brown.^{S5} The r_0 values were taken from the literature^{S6} for calculations performed on V.

Table S5 BVS calculations for the V sites in **1a**.

Vanadium Atoms	BVS			Assigned Oxidation States
	V(III)	V(IV)	V(V)	
V1	3.741	3.886	4.329	IV
V2	3.793	3.937	4.389	IV
V3	3.767	3.909	4.359	IV
V4	3.774	3.918	4.367	IV
V5	3.811	3.964	4.409	IV
V6	3.806	3.953	4.404	IV
V7	3.822	3.969	4.422	IV
V8	3.757	3.896	4.347	IV
V9	3.800	3.950	4.397	IV
V10	3.744	3.886	4.332	IV
V11	3.726	3.870	4.311	IV
V12	3.794	3.939	4.390	IV
V13	3.700	3.843	4.281	IV
V14	3.706	3.854	4.289	IV
V15	3.804	3.945	4.402	IV
V16	3.863	4.010	4.470	IV
V17	3.816	3.954	4.415	IV
V18	3.763	3.910	4.355	IV
V19	3.767	3.913	4.358	IV
V20	3.828	3.974	4.429	IV
V21	3.647	3.791	4.220	IV
V22	3.815	3.957	4.415	IV
V23	3.832	3.981	4.434	IV
V24	3.778	3.926	4.372	IV

Table S6 BVS calculations for the V sites in **1b**.

Vanadium Atoms	BVS			Assigned Oxidation States
	V(III)	V(IV)	V(V)	
V1	3.826	3.974	4.428	IV
V2	3.838	3.981	4.441	IV
V3	3.839	3.988	4.442	IV
V4	3.788	3.943	4.384	IV
V5	3.791	3.945	4.387	IV
V6	3.917	4.069	4.533	IV
V7	3.839	3.984	4.443	IV
V8	3.883	4.031	4.493	IV
V9	3.833	3.990	4.435	IV
V10	3.816	3.963	4.416	IV
V11	3.748	3.902	4.337	IV
V12	3.963	4.111	4.585	IV
V13	3.807	3.948	4.405	IV
V14	3.747	3.895	4.335	IV
V15	3.768	3.919	4.360	IV
V16	3.779	3.924	4.373	IV
V17	3.976	4.131	4.601	IV
V18	3.880	4.032	4.490	IV
V19	3.906	4.059	4.520	IV
V20	3.840	3.995	4.444	IV
V21	3.817	3.959	4.416	IV
V22	3.913	4.076	4.528	IV
V23	3.819	3.972	4.419	IV
V24	3.842	3.993	4.445	IV

Table S7 BVS calculations for the V sites in **2**.

Vanadium Atoms	BVS			Assigned Oxidation States
	V(III)	V(IV)	V(V)	
V1	3.757	3.899	4.347	IV
V2	3.818	3.970	4.417	IV
V3	3.787	3.932	4.382	IV
V4	3.765	3.908	4.357	IV
V5	3.786	3.934	4.381	IV
V6	3.807	3.952	4.405	IV
V7	3.784	3.923	4.378	IV
V8	3.754	3.896	4.344	IV
V9	3.755	3.899	4.346	IV
V10	3.754	3.897	4.344	IV
V11	3.751	3.895	4.341	IV
V12	3.784	3.928	4.379	IV
V13	3.823	3.965	4.423	IV
V14	3.752	3.897	4.342	IV
V15	3.743	3.890	4.331	IV
V16	3.769	3.916	4.362	IV
V17	3.820	3.964	4.421	IV
V18	3.766	3.910	4.358	IV
V19	3.806	3.951	4.404	IV
V20	3.774	3.916	4.367	IV
V21	3.777	3.922	4.371	IV
V22	3.804	3.947	4.402	IV
V23	3.736	3.878	4.323	IV
V24	3.780	3.925	4.374	IV

Table S8 BVS calculations for the V sites in **3**.

Vanadium Atoms	BVS			Assigned Oxidation States
	V(III)	V(IV)	V(V)	
V1	3.074	3.343	3.557	III
V2	3.074	3.342	3.557	III
V3	3.754	3.905	4.343	IV
V4	3.881	4.033	4.491	IV
V5	3.780	3.933	4.374	IV
V6	3.714	3.864	4.298	IV
V7	3.749	3.908	4.338	IV
V8	3.772	3.914	4.365	IV
V9	3.607	3.752	4.174	IV
V10	3.892	4.052	4.504	IV
V11	3.944	4.103	4.564	IV
V12	3.707	3.851	4.289	IV
V13	3.951	4.109	4.571	IV
V14	3.909	4.060	4.523	IV

References

- S1 M. J. Frisch, et al., Gaussian 09, Gaussian, Inc., Wallingford, CT, 2009.
S2 G. M. Sheldrick, *Acta Crystallogr.* 2015, **A71**, 3–8.
S3 G. M. Sheldrick, *Acta Crystallogr.* 2008, **A64**, 112–122.
S4 A. L. Spek, *Acta Crystallogr.* 2015, **C71**, 9–18.
S5 I. D. Brown and D. Altermatt, *Acta Crystallogr. Sect. B*, 1985, **41**, 244–247.
S6 W. Liu and H. H. Thorp, *Inorg. Chem.* 1993, **32**, 4102–4105.